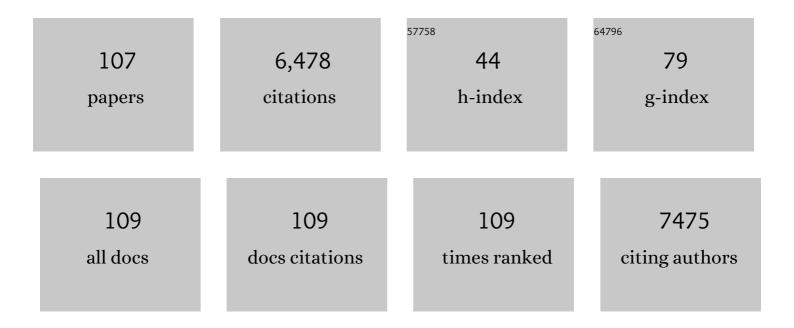


List of Publications by Year in descending order

Source: https://exaly.com/author-pdf/4647419/publications.pdf Version: 2024-02-01



#	Article	IF	CITATIONS
1	Isolation and Identification of Pseudo Seven-Coordinate Ru(III) Intermediate Completing the Catalytic Cycle of Ru-bda Type of Water Oxidation Catalysts. CCS Chemistry, 2022, 4, 2481-2490.	7.8	16
2	Bifunctional spiro-fluorene/heterocycle cored hole-transporting materials: Role of the heteroatom on the photovoltaic performance of perovskite solar cells. Chemical Engineering Journal, 2022, 431, 133371.	12.7	11
3	Effect of the Ancillary Ligand on the Performance of Heteroleptic Cu(I) Diimine Complexes as Dyes in Dye-Sensitized Solar Cells. ACS Applied Energy Materials, 2022, 5, 1460-1470.	5.1	10
4	A Universal Ternaryâ€Solventâ€Ink Strategy toward Efficient Inkjetâ€Printed Perovskite Quantum Dot Lightâ€Emitting Diodes. Advanced Materials, 2022, 34, e2107798.	21.0	109
5	Ocean wave energy generator based on graphene/TiO ₂ nanoparticle composite films. Nanoscale Advances, 2022, 4, 1533-1537.	4.6	0
6	Molecularly Engineered Low-Cost Organic Hole-Transporting Materials for Perovskite Solar Cells: The Substituent Effect on Non-fused Three-Dimensional Systems. ACS Applied Energy Materials, 2022, 5, 3156-3165.	5.1	2
7	A Near-Field Measurement and Calibration Technique: Radio-Frequency Electromagnetic Field Exposure Assessment of Millimeter-Wave 5G Devices. IEEE Antennas and Propagation Magazine, 2021, 63, 77-88.	1.4	17
8	A crosslinked polymer as dopant-free hole-transport material for efficient n-i-p type perovskite solar cells. Journal of Energy Chemistry, 2021, 55, 211-218.	12.9	29
9	Developing D–π–D hole-transport materials for perovskite solar cells: the effect of the π-bridge on device performance. Materials Chemistry Frontiers, 2021, 5, 876-884.	5.9	33
10	Fast Power Density Assessment of 5G Mobile Handset Using Equivalent Currents Method. IEEE Transactions on Antennas and Propagation, 2021, 69, 6857-6869.	5.1	12
11	Morphology and electronic modulation of composite nanosheets for electrocatalytic oxygen evolution through partial and <i>in situ</i> transformation of NiFe-LDH. CrystEngComm, 2021, 23, 1572-1577.	2.6	3
12	Photoinduced defect engineering: enhanced photocatalytic performance of 3D BiOCl nanoclusters with abundant oxygen vacancies. CrystEngComm, 2021, 23, 1305-1311.	2.6	20
13	Lattice distortion in hybrid NiTe2/Ni(OH)2 nanosheets as efficient synergistic electrocatalyst for water and urea oxidation. Journal of Power Sources, 2020, 449, 227585.	7.8	40
14	Design, Synthesis, and Photocatalytic Application of Moisture-Stable Hybrid Lead-Free Perovskite. ACS Applied Materials & Interfaces, 2020, 12, 54694-54702.	8.0	36
15	Low-temperature carbon-based electrodes in perovskite solar cells. Energy and Environmental Science, 2020, 13, 3880-3916.	30.8	149
16	Hierarchical Z-scheme Fe ₂ O ₃ @ZnIn ₂ S ₄ core–shell heterostructures with enhanced adsorption capacity enabling significantly improved photocatalytic CO ₂ reduction. CrystEngComm, 2020, 22, 8221-8227.	2.6	15
17	Triplex Glass Laminates with Silicon Quantum Dots for Luminescent Solar Concentrators. Solar Rrl, 2020, 4, 2000195.	5.8	31
18	Hierarchical Ni-BDC coated FeOOH nanosheets: A coordination tuning synergistic electrocatalyst with enhanced activity for water oxidation. International Journal of Hydrogen Energy, 2020, 45, 9546-9554.	7.1	5

#	Article	IF	CITATIONS
19	Organic Salts as p-Type Dopants for Efficient LiTFSI-Free Perovskite Solar Cells. ACS Applied Materials & Interfaces, 2020, 12, 33751-33758.	8.0	24
20	Single crystal structure and opto-electronic properties of oxidized Spiro-OMeTAD. Chemical Communications, 2020, 56, 1589-1592.	4.1	24
21	Impact of Linking Topology on the Properties of Carbazoleâ€Based Holeâ€Transport Materials and their Application in Solidâ€State Mesoscopic Solar Cells. Solar Rrl, 2019, 3, 1900196.	5.8	17
22	Exploring the Optical and Electrochemical Properties of Homoleptic versus Heteroleptic Diimine Copper(I) Complexes. Inorganic Chemistry, 2019, 58, 12167-12177.	4.0	25
23	Bimetallic metal-organic framework derived electrocatalyst for efficient overall water splitting. International Journal of Hydrogen Energy, 2019, 44, 5983-5989.	7.1	26
24	A heavy metal-free CuInS ₂ quantum dot sensitized NiO photocathode with a Re molecular catalyst for photoelectrochemical CO ₂ reduction. Chemical Communications, 2019, 55, 7918-7921.	4.1	21
25	An Indacenodithieno[3,2â€b]thiopheneâ€Based Organic Dye for Solidâ€State pâ€Type Dyeâ€Sensitized Solar Ce ChemSusChem, 2019, 12, 3243-3248.	^{lls} . 6.8	13
26	Constructing moisture-stable hybrid lead iodine semiconductors based on hydrogen-bond-free and dual-iodine strategies. Journal of Materials Chemistry C, 2019, 7, 7700-7707.	5.5	11
27	Over 12% Efficiency Nonfullerene Allâ€Smallâ€Molecule Organic Solar Cells with Sequentially Evolved Multilength Scale Morphologies. Advanced Materials, 2019, 31, e1807842.	21.0	272
28	Optically Transparent Wood Substrate for Perovskite Solar Cells. ACS Sustainable Chemistry and Engineering, 2019, 7, 6061-6067.	6.7	89
29	Solution-processed nanoporous NiO-dye-ZnO photocathodes: Toward efficient and stable solid-state p-type dye-sensitized solar cells and dye-sensitized photoelectrosynthesis cells. Nano Energy, 2019, 55, 59-64.	16.0	36
30	CHAPTER 3. Dye-sensitised Solar Cells. Inorganic Materials Series, 2019, , 89-152.	0.7	1
31	A-D-A Structured Small-Molecule Hole Transporting Materials for Dopant-Free Perovskite Solar Cells. General Chemistry, 2019, 5, 180026-180026.	0.6	0
32	Spectrum-enhanced Au@ZnO plasmonic nanoparticles for boosting dye-sensitized solar cell performance. Journal of Power Sources, 2018, 380, 142-148.	7.8	27
33	RF Compliance Study of Temperature Elevation in Human Head Model Around 28 GHz for 5G User Equipment Application: Simulation Analysis. IEEE Access, 2018, 6, 830-838.	4.2	51
34	Pd@MIL-100(Fe) composite nanoparticles as efficient catalyst for reduction of 2/3/4-nitrophenol: Synergistic effect between Pd and MIL-100(Fe). Microporous and Mesoporous Materials, 2018, 255, 1-6.	4.4	66
35	Molecular Engineering of Dâ^'ï€â€"A Type of Blue-Colored Dyes for Highly Efficient Solid-State Dye-Sensitized Solar Cells through Co-Sensitization. ACS Applied Materials & Interfaces, 2018, 10, 35946-35952.	8.0	8
36	The Importance of Pendant Groups on Triphenylamineâ€Based Hole Transport Materials for Obtaining Perovskite Solar Cells with over 20% Efficiency. Advanced Energy Materials, 2018, 8, 1701209.	19.5	134

#	Article	IF	CITATIONS
37	Facile and large-scale preparation of Co/Ni-MoO2 composite as high-performance electrocatalyst for hydrogen evolution reaction. International Journal of Hydrogen Energy, 2018, 43, 20721-20726.	7.1	23
38	Chemical Dopant Engineering in Hole Transport Layers for Efficient Perovskite Solar Cells: Insight into the Interfacial Recombination. ACS Nano, 2018, 12, 10452-10462.	14.6	78
39	D–A–D-Typed Hole Transport Materials for Efficient Perovskite Solar Cells: Tuning Photovoltaic Properties via the Acceptor Group. ACS Applied Materials & Interfaces, 2018, 10, 19697-19703.	8.0	101
40	Diâ€Spiroâ€Based Holeâ€Transporting Materials for Highly Efficient Perovskite Solar Cells. Advanced Energy Materials, 2018, 8, 1800809.	19.5	79
41	Ternary non-fullerene polymer solar cells with 13.51% efficiency and a record-high fill factor of 78.13%. Energy and Environmental Science, 2018, 11, 3392-3399.	30.8	143
42	Efficient Dye-Sensitized Solar Cells with Voltages Exceeding 1 V through Exploring Tris(4-alkoxyphenyl)amine Mediators in Combination with the Tris(bipyridine) Cobalt Redox System. ACS Energy Letters, 2018, 3, 1929-1937.	17.4	22
43	Covalently linking CuInS ₂ quantum dots with a Re catalyst by click reaction for photocatalytic CO ₂ reduction. Dalton Transactions, 2018, 47, 10775-10783.	3.3	37
44	Design and synthesis of dopant-free organic hole-transport materials for perovskite solar cells. Chemical Communications, 2018, 54, 9571-9574.	4.1	49
45	Molecular engineering of D–A–π–A sensitizers for highly efficient solid-state dye-sensitized solar cells. Journal of Materials Chemistry A, 2017, 5, 3157-3166.	10.3	41
46	Design, synthesis and application of a π-conjugated, non-spiro molecular alternative as hole-transport material for highly efficient dye-sensitized solar cells and perovskite solar cells. Journal of Power Sources, 2017, 344, 11-14.	7.8	49
47	Incorporation of Counter Ions in Organic Molecules: New Strategy in Developing Dopantâ€Free Hole Transport Materials for Efficient Mixedâ€Ion Perovskite Solar Cells. Advanced Energy Materials, 2017, 7, 1602736.	19.5	72
48	Tailor-Making Low-Cost Spiro[fluorene-9,9′-xanthene]-Based 3D Oligomers for Perovskite Solar Cells. CheM, 2017, 2, 676-687.	11.7	222
49	Novel and Stable D–Aâ^'π–A Dyes for Efficient Solid-State Dye-Sensitized Solar Cells. ACS Omega, 2017, 2, 1812-1819.	3.5	19
50	Understandings of maximum spatially-averaged power density in 5G RF EMF exposure study. , 2017, , .		4
51	Glycol assisted synthesis of MIL-100(Fe) nanospheres for photocatalytic oxidation of benzene to phenol. Catalysis Communications, 2017, 98, 112-115.	3.3	51
52	High performance solid-state dye-sensitized solar cells based on organic blue-colored dyes. Journal of Materials Chemistry A, 2017, 5, 1242-1247.	10.3	35
53	Power Density Measurements at 15 GHz for RF EMF Compliance Assessments of 5G User Equipment. IEEE Transactions on Antennas and Propagation, 2017, 65, 6584-6595.	5.1	46
54	Direct selenylation of mixed Ni/Fe metal-organic frameworks to NiFe-Se/C nanorods for overall water splitting. Journal of Power Sources, 2017, 366, 193-199.	7.8	72

#	Article	IF	CITATIONS
55	Rapid and Efficient Self-Assembly of Au@ZnO Core–Shell Nanoparticle Arrays with an Enhanced and Tunable Plasmonic Absorption for Photoelectrochemical Hydrogen Generation. ACS Applied Materials & Interfaces, 2017, 9, 31897-31906.	8.0	53
56	4â€ <i>Tert</i> â€butylpyridine Free Organic Hole Transporting Materials for Stable and Efficient Planar Perovskite Solar Cells. Advanced Energy Materials, 2017, 7, 1700683.	19.5	115
57	Sandwich-like MIL-100(Fe)@Pt@MIL-100(Fe) nanoparticles for catalytic hydrogenation of 4-nitrophenol. Catalysis Communications, 2017, 102, 17-20.	3.3	14
58	RF EMF exposure of beam-steering slot array in 5g user equipment at 15 GHz. , 2017, , .		1
59	Novel Ni(S0.49Se0.51)2 porous flakes array on carbon fiber cloth for efficient hydrogen evolution reaction. International Journal of Hydrogen Energy, 2017, 42, 30119-30125.	7.1	22
60	Highly Efficient Porphyrinâ€Based OPV/Perovskite Hybrid Solar Cells with Extended Photoresponse and High Fill Factor. Advanced Materials, 2017, 29, 1703980.	21.0	176
61	Constructive Effects of Alkyl Chains: A Strategy to Design Simple and Nonâ€Spiro Hole Transporting Materials for Highâ€Efficiency Mixedâ€Ion Perovskite Solar Cells. Advanced Energy Materials, 2016, 6, 1502536.	19.5	72
62	Facile synthesized organic hole transporting material for perovskite solar cell with efficiency of 19.8%. Nano Energy, 2016, 23, 138-144.	16.0	253
63	Facile synthesis of fluorene-based hole transport materials for highly efficient perovskite solar cells and solid-state dye-sensitized solar cells. Nano Energy, 2016, 26, 108-113.	16.0	103
64	Aqueous controllable synthesis of spindle-like palladium nanoparticles and their application for catalytic reduction of 4-nitrophenol. Progress in Natural Science: Materials International, 2016, 26, 295-302.	4.4	12
65	Investigation of surface waves suppression on 5G handset devices at 15 GHz. , 2016, , .		1
66	The Role of 3D Molecular Structural Control in New Hole Transport Materials Outperforming <i>Spiro</i> â€OMeTAD in Perovskite Solar Cells. Advanced Energy Materials, 2016, 6, 1601062.	19.5	87
67	Strategy to Boost the Efficiency of Mixed-Ion Perovskite Solar Cells: Changing Geometry of the Hole Transporting Material. ACS Nano, 2016, 10, 6816-6825.	14.6	127
68	A novel 2D porous indium coordination polymer with tunable luminescent property. Journal of Molecular Structure, 2016, 1118, 105-109.	3.6	5
69	High conductivity Ag-based metal organic complexes as dopant-free hole-transport materials for perovskite solar cells with high fill factors. Chemical Science, 2016, 7, 2633-2638.	7.4	89
70	A low-cost spiro[fluorene-9,9′-xanthene]-based hole transport material for highly efficient solid-state dye-sensitized solar cells and perovskite solar cells. Energy and Environmental Science, 2016, 9, 873-877.	30.8	362
71	A study of oligothiophene–acceptor dyes in p-type dye-sensitized solar cells. RSC Advances, 2016, 6, 18165-18177.	3.6	21
72	Preparation and photocatalytic property of spindle-like MIL-88B(Fe) nanoparticles. Inorganic Chemistry Communication, 2016, 67, 29-31.	3.9	51

#	Article	IF	CITATIONS
73	Dye-Sensitized Solar Cells: 1,1,2,2-Tetrachloroethane (TeCA) as a Solvent Additive for Organic Hole Transport Materials and Its Application in Highly Efficient Solid-State Dye-Sensitized Solar Cells (Adv.) Tj ETQq1	10.728431	4 rgBT /Over
74	Phenoxazineâ€Based Small Molecule Material for Efficient Perovskite Solar Cells and Bulk Heterojunction Organic Solar Cells. Advanced Energy Materials, 2015, 5, 1401720.	19.5	109
75	Structure and function relationships in alkylammonium lead(<scp>ii</scp>) iodide solar cells. Journal of Materials Chemistry A, 2015, 3, 9201-9207.	10.3	57
76	1,1,2,2â€Tetrachloroethane (TeCA) as a Solvent Additive for Organic Hole Transport Materials and Its Application in Highly Efficient Solidâ€State Dyeâ€Sensitized Solar Cells. Advanced Energy Materials, 2015, 5, 1402340.	19.5	57
77	Novel Small Molecular Materials Based on Phenoxazine Core Unit for Efficient Bulk Heterojunction Organic Solar Cells and Perovskite Solar Cells. Chemistry of Materials, 2015, 27, 1808-1814.	6.7	100
78	Organic Dye-Sensitized Tandem Photoelectrochemical Cell for Light Driven Total Water Splitting. Journal of the American Chemical Society, 2015, 137, 9153-9159.	13.7	327
79	Synthesis, Crystal Structures, and Luminescent Properties of Two Complexes based on 5â€ <i>tert</i> â€Butylisophthalic Acid and 1, 2â€Bis(4â€pyridyl) Ethane. Zeitschrift Fur Anorganische Und Allgemeine Chemie, 2015, 641, 1311-1315.	1.2	6
80	A novel phenoxazine-based hole transport material for efficient perovskite solar cell. Journal of Energy Chemistry, 2015, 24, 698-706.	12.9	22
81	The combination of a new organic D–π–A dye with different organic hole-transport materials for efficient solid-state dye-sensitized solar cells. Journal of Materials Chemistry A, 2015, 3, 4420-4427.	10.3	45
82	Structure and photocatalytic property of a new Cu(II) based framework with jsm topology. Inorganic Chemistry Communication, 2015, 52, 9-11.	3.9	4
83	Integrated Design of Organic Hole Transport Materials for Efficient Solidâ€State Dyeâ€Sensitized Solar Cells. Advanced Energy Materials, 2015, 5, 1401185.	19.5	59
84	EFFECT OF THE CHROMOPHORES STRUCTURES ON THE PERFORMANCE OF SOLID-STATE DYE SENSITIZED SOLAR CELLS. Nano, 2014, 09, 1440005.	1.0	7
85	Syntheses, crystal and band structures, and optical properties of a selenidoantimonate and an iron polyselenide. Journal of Solid State Chemistry, 2014, 218, 109-115.	2.9	7
86	Solid‧tate Perovskite‧ensitized pâ€Type Mesoporous Nickel Oxide Solar Cells. ChemSusChem, 2014, 7, 2150-2153.	6.8	69
87	Two novel Pb(II)-based heterometallic coordination polymers assembled from 1,3,5-benzenetricarboxylic acid: Syntheses, structures and luminescent properties. Journal of Molecular Structure, 2014, 1059, 320-324.	3.6	14
88	Structure and luminescent property of a zinc(II) complex assembled from 5-methylisophthalic acid and 1,2-bis-(4-pyridyl) ethane. Journal of Molecular Structure, 2014, 1056-1057, 52-55.	3.6	4
89	Improved Performance of Colloidal CdSe Quantum Dot-Sensitized Solar Cells by Hybrid Passivation. ACS Applied Materials & Interfaces, 2014, 6, 18808-18815.	8.0	36
90	Structures and properties of four coordination polymers constructed from 1,3-bis-(4-pyridyl)-propane and aromatic dicarboxylic acids. RSC Advances, 2014, 4, 13919.	3.6	8

#	Article	IF	CITATIONS
91	Two novel Ni(II) complexes with polycatenated networks: Structures and magnetic properties. Inorganic Chemistry Communication, 2014, 47, 119-122.	3.9	9
92	Structural and functional studies on coordination polymers based on 5-tert-butylisophthalic acid and N,N′-bis-(4-pyridylmethyl) piperazine. RSC Advances, 2014, 4, 25588.	3.6	6
93	Carbazoleâ€Based Holeâ€Transport Materials for Efficient Solidâ€State Dyeâ€Sensitized Solar Cells and Perovskite Solar Cells. Advanced Materials, 2014, 26, 6629-6634.	21.0	369
94	AgTFSI as pâ€Type Dopant for Efficient and Stable Solidâ€State Dyeâ€Sensitized and Perovskite Solar Cells. ChemSusChem, 2014, 7, 3252-3256.	6.8	114
95	A Yb(III)–Zn(II) heterometallic coordination polymer with interesting three-fold 1D pseudo-nanotube architectures. Journal of Molecular Structure, 2014, 1068, 53-57.	3.6	0
96	Structures and Properties of Coordination Polymers based on 5â€Nitroisophthalic Acid and <i>N</i> , <i>N</i> ′â€bis(4â€pyridylâ€methyl) Piperazine. Zeitschrift Fur Anorganische Und Allgemeine Chemie, 2014, 640, 2503-2507.	1.2	5
97	Enhancement of p-Type Dye-Sensitized Solar Cell Performance by Supramolecular Assembly of Electron Donor and Acceptor. Scientific Reports, 2014, 4, 4282.	3.3	59
98	Efficient solid state dye-sensitized solar cells based on an oligomer hole transport material and an organic dye. Journal of Materials Chemistry A, 2013, 1, 14467.	10.3	67
99	Initial Light Soaking Treatment Enables Hole Transport Material to Outperform Spiro-OMeTAD in Solid-State Dye-Sensitized Solar Cells. Journal of the American Chemical Society, 2013, 135, 7378-7385.	13.7	138
100	Bistriphenylamine-substituted fluoranthene derivatives as electroluminescent emitters and dye-sensitized solar cells. Tetrahedron, 2012, 68, 10372-10377.	1.9	8
101	Colorâ€Tunable Solidâ€State Emission of 2,2′â€Biindenylâ€Based Fluorophores. Angewandte Chemie - International Edition, 2011, 50, 11654-11657.	13.8	254
102	Unsymmetrically amorphous 9,10-disubstituted anthracene derivatives for high-efficiency blue organic electroluminescence devices. Dyes and Pigments, 2011, 89, 155-161.	3.7	27
103	New photochromic chemosensors for Hg2+ and Fâ^'. Tetrahedron, 2011, 67, 915-921.	1.9	90
104	Ground and excited states calculations of 7-phenylamino-substituted coumarins. Journal of Molecular Structure, 2009, 917, 15-20.	3.6	12
105	Modeling of Overflow Metabolism in Batch and Fed-Batch Cultures of Escherichia coli. Biotechnology Progress, 1999, 15, 81-90.	2.6	169
106	Monitoring of genes that respond to process-related stress in large-scale bioprocesses. Biotechnology and Bioengineering, 1999, 65, 151-159.	3.3	124
107	Continuous measurement of NOaq during denitrification by immobilized Pseudomonas stutzeri. Biotechnology Letters, 1995, 9, 659-664.	0.5	4